MRI-GUIDED prostate motion tracking by means of multislice-to-volume registration

Hadi Tadayyon[a], Siddharth Vikal[b], Sean Gill[b], Andras Lasso[b], and Gabor Fichtinger[a,b]
[a]Dept. of Electrical & Computer Engineering, Queen's University, Kingston, Canada K7L 3N6
[b]School of Computing, Queen's University, Kingston, Canada K7L 3N6

ABSTRACT

We developed an algorithm for tracking prostate motion during MRI-guided prostatic needle placement, with the primary application in prostate biopsy. Our algorithm has been tested on simulated patient and phantom data. The algorithm features a robust automatic restart and a 12-core biopsy error validation scheme. Simulation tests were performed on four patient MRI pre-operative volumes. Three orthogonal slices were extracted from the pre-operative volume to simulate the intra-operative volume and a volume of interest was defined to isolate the prostate. Phantom tests used six datasets, each representing the phantom at a known perturbed position. These volumes were registered to their corresponding reference volume (the phantom at its home position). Convergence tests on the phantom data showed that the algorithm demonstrated accurate results at 100% confidence level for initial misalignments of less than 5mm and at 73% confidence level for initial misalignments less than 10mm. Our algorithm converged in 95% of the cases for the simulated patient data with 0.66mm error and the six phantom registration tests resulted in 1.64mm error.

Keywords: Slice-to-volume registration, MRI, motion tracking, prostate, biopsy

1. INTRODUCTION

Magnetic Resonance Imaging (MRI) is increasingly becoming the modality of choice in guiding percutaneous surgery[1-3]. MRI is suitable in interventional imaging due to its radiation-free environment, high soft-tissue contrast, and its capabilities of advanced imaging including functional MRI (fMRI) and MR spectroscopy[4]. MR imaging of the human prostate is especially of high interest in biopsy planning due to the clear prostate contour.

During a prostate biopsy procedure, the prostate moves with the insertion and retraction of the biopsy needle. This creates the need for a system to track the prostate position throughout the biopsy procedure by computing its new position after each tissue sample extraction. As this computation must be performed during the intervention, registration speed is an important factor in the design of the tracking software. Slice-to-volume[1] registration provides the speed lacked by volume-to-volume registration, due to fewer intra-operative (intra-op) acquisitions and reduced regions of similarity metric computation.

The problem of organ motion tracking under MRI guidance has been explored previously by several groups. (Fei, *et al.* 2003)[5] developed a slice-to-volume registration algorithm with application to radio-frequency thermal ablation of prostate cancer, in which 15 actual interventional MRI (iMRI) slices from transverse, sagittal, and coronal orientations were registered to a pre-operative (pre-op) MRI volume, respectively. The 15 slices from each orientation were independently registered to the pre-op volume, meaning that three independent registrations were performed and the results were compared. Their algorithm featured a multi-resolution approach with an automatic restart. They attained a mean registration time of 15s and an accuracy of 0.4mm using simulated iMRI and 1mm using actual MRI. A more recent work in the field of intra-operative tracking was by (Chandler *et al.* 2006)[6], who corrected for misaligned cardiac anatomy by means of slice-to-volume registration. They achieved a mean registration error of 1.5mm with a registration

[1] Please note that "multi-slice-to-volume" registration is referred for convenience as simply "slice-to-volume" registration for the rest of this paper

Medical Imaging 2010: Visualization, Image-Guided Procedures, and Modeling, edited by Kenneth H. Wong, Michael I. Miga, Proc. of SPIE Vol. 7625, 76252V · © 2010 SPIE · CCC code: 1605-7422/10/$18 · doi: 10.1117/12.844454

time of 2 min. The slower registration time was due to the large number of tracking slices and computationally expensive metric (mutual information). The problem of local extreme traps and the inefficiency of (Fei *et al*. 2003)'s optimization was attacked by (Gill *et al.* 2008)[7], who eliminated the need for a restart routine by performing a multi-resolution registration alone on a volume of interest (VOI), and incorporated transverse and sagittal slices centered around the prostate, which were formed into a simulated intra-op volume. (Gill *et al.* 2008)'s algorithm converged in 107s with 0.75mm error. Out of all the above mentioned works in the literature, three orthogonal slices has not been used for prostate tracking. In this paper, we propose a three orthogonal slice approach to intra-op prostate motion tracking under MRI guidance validated with simulated patient and phantom studies. This will be accomplished by acquiring three orthogonal high-resolution MRI slices of the lower abdomen intermittently and registering them to a high-resolution pre-op volume. In prostate biopsy, as the needle placement causes edematic swelling of the prostate, its deformation after needle insertion may be necessary to be taken into account in registration. However, our rigid registration is based on the assumption that there is no significant prostate deformation during the biopsy procedure and that rigid registration of a post-needle insertion image to pre-needle insertion image will converge to a clinically reasonable error (about 2mm).

Our clinical goal is to accurately and quickly register high-resolution intra-op/iMRI slices to high-resolution pre-op MRI volume of a patient's prostate. In the context of this paper, "accurate" is defined as a registration error of less than 2mm, which is greater than the diameter of a standard biopsy needle (1.2mm)[8] but smaller than the diameter of the clinically significant size of prostate cancer (4mm)[7]. The objective of our tracking is to ascertain current patient position prior to firing the biopsy needle. Tracking is initiated by the physician, requesting the operator to acquire tracking (intra-op) images. Thus, there is a 1-2min delay in the physician's request to obtaining the slices in the tracking software. In this light, our objective for speed is to develop an algorithm fast enough to respond to the physician's acquisition requests timely.

Our proposed approach to MR-guided intra-op prostate motion tracking is different from (Gill *et al.* 2008)'s approach in several ways. First, we created an automatic restart routine which does not depend on a multi-resolution approach. Second, the simulated iMRI slices have the same thickness and spacing as the pre-op slices and there is no slice averaging as performed by (Gill *et al.* 2008). It is assumed that the iMRI scans are acquired at the same thickness and spacing as the high-resolution pre-op scans, which is reasonable as only three slices are needed for the intra-op volume. Third, we added a third orthogonal slice to the simulated iMRI volume to increase accuracy. Fourth, we used a more representative error validation scheme whereby the average Euclidian distance error between the reference point and the registered point were measured at 12 realistic biopsy locations based on a 12-core biopsy method which will be described in more detail in section 3. Fifth, we conducted phantom studies to test our algorithm on real intra-op images, which was lacked by (Gill *et al.* 2008). Lastly, our tracking algorithm was developed using the Insight Segmentation and Registration Toolkit (ITK) which generally performs registration and segmentation significantly faster than MATLAB's image processing toolbox. The following sections will describe the details of the registration technique.

2. METHODOLOGY

2.1 Program Workflow

The first stage of our work was to develop and test the slice-to-volume registration method using simulated intra-op slices, to determine the overall feasibility of this tracking method. Clinical patient data prior to needle insertion was used as the ground-truth volume, which is referred to as the pre-op volume throughout this paper. The intra-op volume was formed by extracting three orthogonal slices from the center of the pre-op prostate volume and treating these slices as a sparse volume. Next, a VOI was defined covering the prostate in the intra-op volume to prevent the surrounding bones and tissues from affecting the registration. The pre-op volume was computationally perturbed by a known 6 degree of freedom (DOF) transformation and the goal of the registration was to find the pre-op volume's way back home, which is the origin of the intra-op volume. Registration was restarted with random adjustment of the transformation parameters. Details of the restart routine will be discussed in section 2.3. The main difference between the setup of the phantom registration and the patient simulation experiment is that the intra-op volume for the phantom registration was real, acquired after translating/rotating the phantom by a known amount. Figure 1 illustrates how the fixed and moving images were formed for the two registration tests. Naturally, our tracking algorithm can be integrated with a navigation

system or a needle placement robot (with the appropriate driver software and hardware) to automatically control the position of the needle.

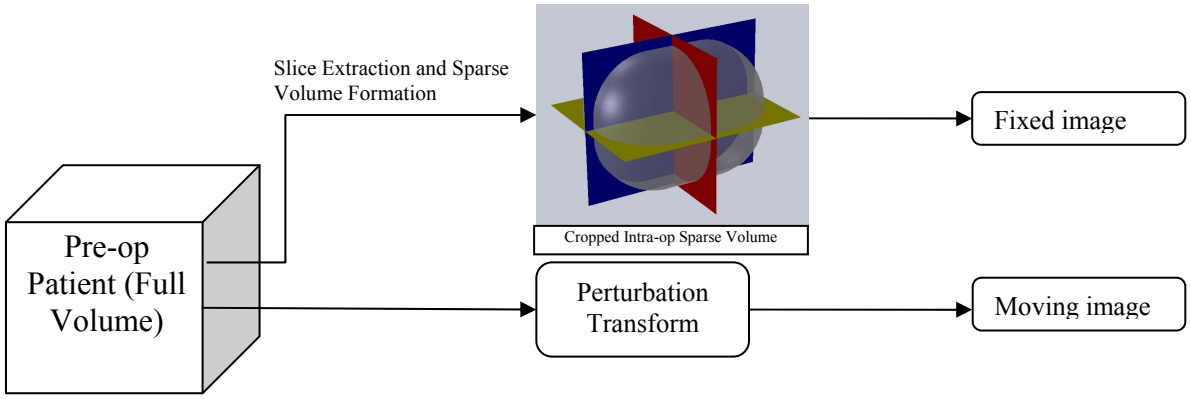

Figure 1a: Image pre-processing and input setup for the simulated registration

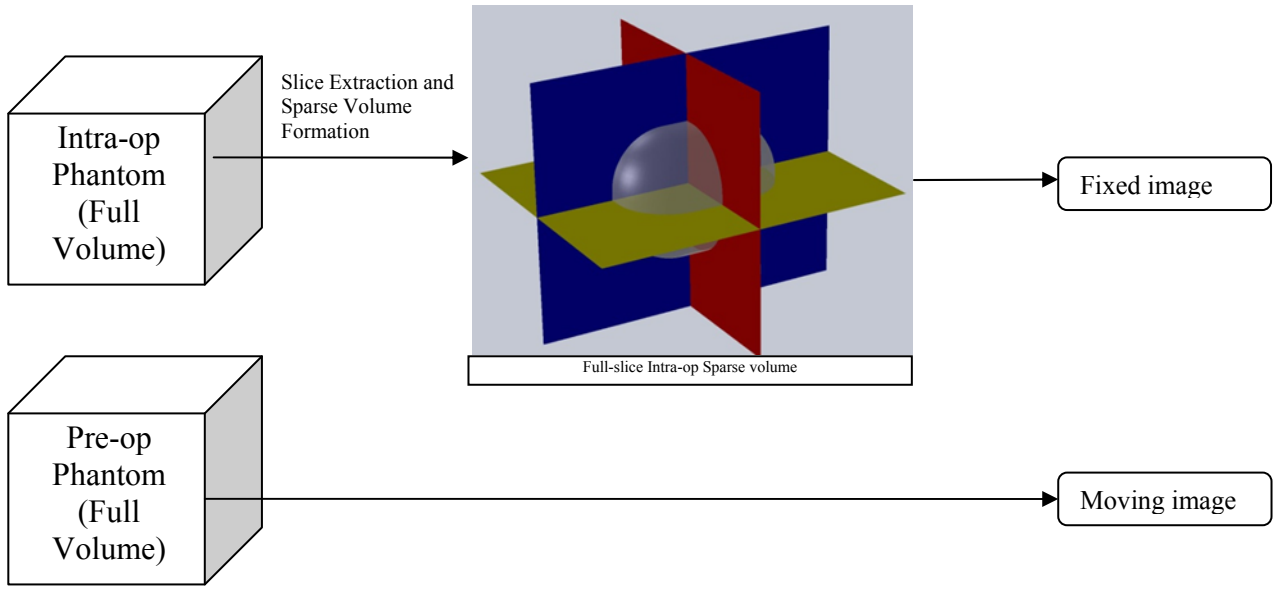

Figure 1b: Image pre-processing and input setup for the phantom registration

2.2 Volumes of Interest

For the patient simulations, the fixed image was selected as a sparse volume, which was a volume enclosing the prostate consisting of 3 slices extracted from the pre-op volume – 1 transverse, 1 sagittal, and 1 coronal, all cutting through the center of mass of the prostate. As previously mentioned, a VOI was defined for the fixed image (intra-op volume), which was constructed manually without any automatic segmentation to save pre-registration time. For each patient, the extents of the prostate in each dimension X, Y, and Z, and the coordinate location of the endorectal coil center were found from the image by manual inspection. The above mentioned four parameters were part of the input to our program, which were used for constructing the VOI.

A VOI was defined enclosing the phantom prostate and half of the rectum. Some of the rectum was required in the VOI in order to assist the registration, acting as a fiducial. However, the rectum was not included in the patient VOI as it was predicted that the patient prostate has enough anatomical features to allow the registration algorithm to converge.

2.3 Registration Components

The mapping of the moving image voxels to the fixed image space after applying a transformation was determined by linear interpolation. The metric used was a mean squares metric, which computes the mean square of the intensity differences over the three regions of the prostate (the three slices) in the two images, ignoring the empty voxels between the slices. The mean squares metric was chosen because it is one of the fastest metrics to compute and is most suitable for unimodal applications. The registration problem is a 6 DOF optimization problem, which involves 3 rotations about and 3 translations along X, Y, and Z axes, respectively.

2.4 Optimization

We extended ITK's original optimization algorithm by adding an automatic optimization restart routine to guide the optimizer away from local minima. At the end of each iteration, a random perturbation was added to the registration parameters and the resulting new transformation was fed to the next registration attempt as the new initial guess. The registration was restarted 5 times and the registration parameters resulting from the smallest cost function out of the five cost functions was selected as the final result of the registration.

3. DATA

For the patient simulation, high-resolution pre-op MRI volumes were acquired from a T2 MRI transverse scan using a 1.5T GE MRI system. The images had resolutions of 0.625 x 0.625 x 3 mm/pixel for Patients 1, 3, and 4, and 0.78 x 0.78 x 4 mm/pixel for Patient 2. The patient lied in prone position, then a transrectal probe was inserted through the patient's rectum, and transverse MR slices were acquired as the probe advanced incrementally through the rectum. Four MRI acquisitions from four patients were used in our simulation experiments. Although the acquired slices can be transverse, sagittal, or coronal, incorporation of the transverse slice as the highest resolution slice in a slice-to-volume registration problem was proven in a previous study[5] to be beneficial and yield the best results for MR images as compared to the other two orientations.

The phantom images were all acquired at 0.625 x 0.625 x 3 mm/pixel resolution. The moving image was a high-resolution phantom volume at the reference position and the fixed image was a sparse volume created in the same manner as the simulation, with the orthogonal slices extracted from a high-resolution volume of the perturbed phantom (actual image, not simulated).

4. EXPERIMENTS AND RESULTS

To compute the registration error, 12 biopsy points were selected on the pre-op prostate volume. The biopsy locations were chosen based on the standard sextant prostate biopsy method plus six points in the peripheral zone (three on each side)[10]. The biopsy locations are illustrated in The fourth phantom test case (fourth column of table 2) was included in the results since the initial displacement was close to 10mm and it allowed for testing the limits of the algorithm.
2. The RAS[2] coordinates of the biopsy points in the transformed pre-op volume's frame relative to the original pre-op volume's frame were computed using the transformation matrix obtained from the registration. Then the Euclidian distance between the transformed point and the original point was calculated for each biopsy point. The registration error was defined as the average of the 12 Euclidian distance errors for each perturbation case. The overall registration error recorded in table 1 for each data set represents the average of the 25 registration errors calculated for the 25 perturbations.

[2] **R**ight-left, **A**nterior-posterior, **S**uperior-inferior is the standard coordinate system used in clinical settings which defines the location of the subject (usually the patient) relative to a fixed point (such as a point on the patient bed).

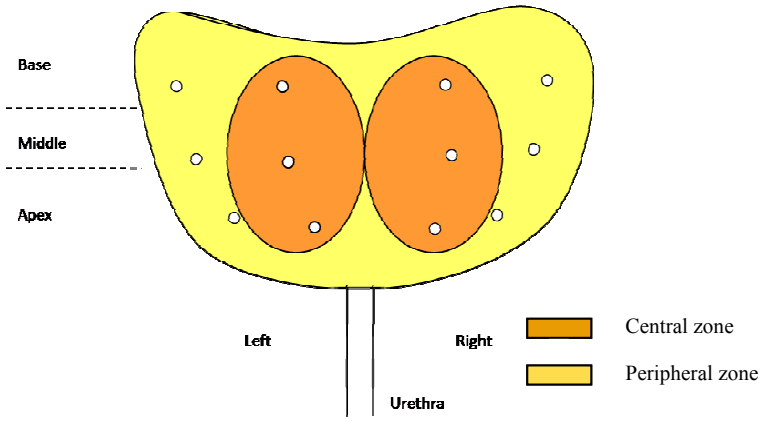

Figure 2: Biopsy locations chosen for measuring registration error

For the simulation, our algorithm was tested with 25 perturbations per data set for a total of 100 registrations. The perturbation used for simulating the displacement of the prostate was given by a uniform distribution of random numbers. An array containing 25 random translations between -5mm and +5mm and 25 random rotations in the range of -5^{o} to $+5^{o}$ was generated and input to the algorithm. Before applying the perturbation, the misalignment resulting from the current perturbation values was computed by measuring the average displacement of the biopsy targets. If the misalignment was below 10mm, the perturbation was used for the registration, otherwise, it was discarded and another set of random translations and rotations were generated, and the process was repeated. This was implemented to generate realistic perturbation data and was based on the assumption that the average intra-operative displacement of biopsy targets does not exceed 10mm in the clinical procedure. Registration succeeded 95% of the time. The registration errors are shown in Table 1.

The phantom experiment consisted of a two-phase test. The first phase was a simulation experiment, whereby the intra-op volume was simulated from the pre-op phantom volume, in a similar manner to the patient simulation experiment. Registrations were performed for 75 random perturbations, using the same ranges as the patient simulation case. This test was conducted first to evaluate the convergence range of our phantom images, for which a histogram was plotted from the test results, which is shown in Figure 3. The histogram shows the percentage of cases that successfully converged for a particular bin of initial registration error (iRE), where successful convergence was defined as a final registration error (fRE) of less than 0.5mm. A threshold of 0.5mm was used rather than 2mm for two reasons. First, for the patient simulations the transformed images were computationally created, therefore the ground truth displacement was fully known, and so a stricter pass/fail condition can be applied for the registration accuracy validation. Second, all simulation cases resulted in less than 2mm error, and thus, using a threshold of 2mm would mean that all 75 tests converged, which would render the convergence histogram meaningless. It seemed intuitive to use 0.5mm as this was the average final registration error among the simulation tests and produced a realistic histogram. In the second test phase, we replaced the simulated intra-op volume with the actual intra-op volume, and performed registrations on six different volumes of the same phantom, each acquired after a known perturbation. However, the perturbation parameters were only known in the physical coordinate system of the experimental setup, which was not known to us. Thus, our ground truth was found by using image analysis software by manually registering the two volumes in a trial-and-error manner. The resulting transformation, after a manual registration, was defined as our ground truth, and the transformations obtained by the algorithm were compared against the ground truth to determine the registration error. The initial registration error (RE) values in table 2 represent the initial misalignment based on the ground truth transformation found from the manual registrations we performed initially. A checkerboard overlay of the intra-op and pre-op phantom volumes is shown in Figure 4 for the case where the phantom was rotated -5^{0} about the X axis relative to the physical coordinate system. This physical rotation translated to a misalignment of [-5, 0, 0, -2, -1, 15] in the coordinate system defined in our programming environment, where the first three parameters represent the rotations (degrees) and the last three represent the translations(mm). The existence of translations in the misalignment was due to the different centers of rotation defined in the physical and the program's coordinate systems. The corresponding intra-op and pre-op slices are overlaid in the three orthogonal views and are shown pre-registration and post-registration.

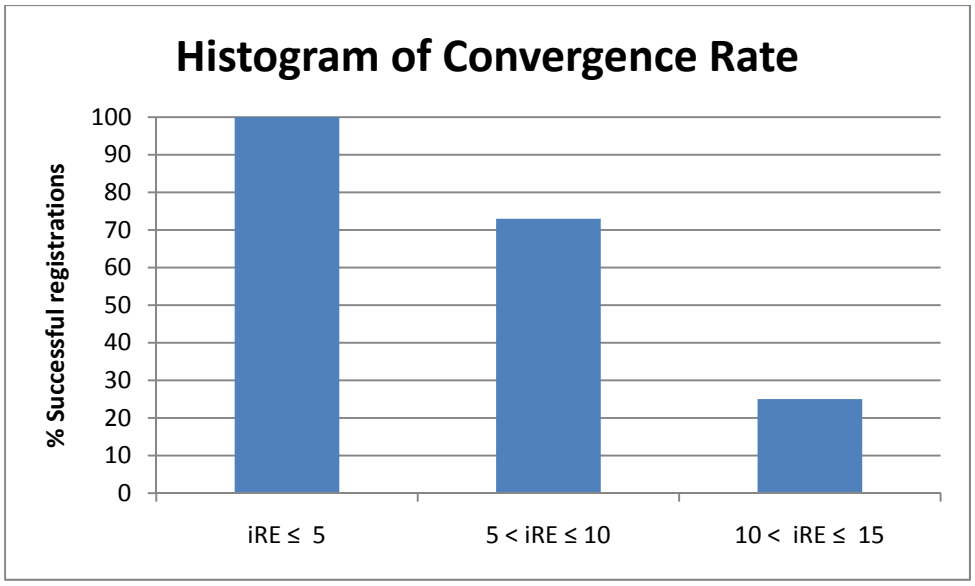

Figure 3: Histogram of convergence rate for phantom experiments

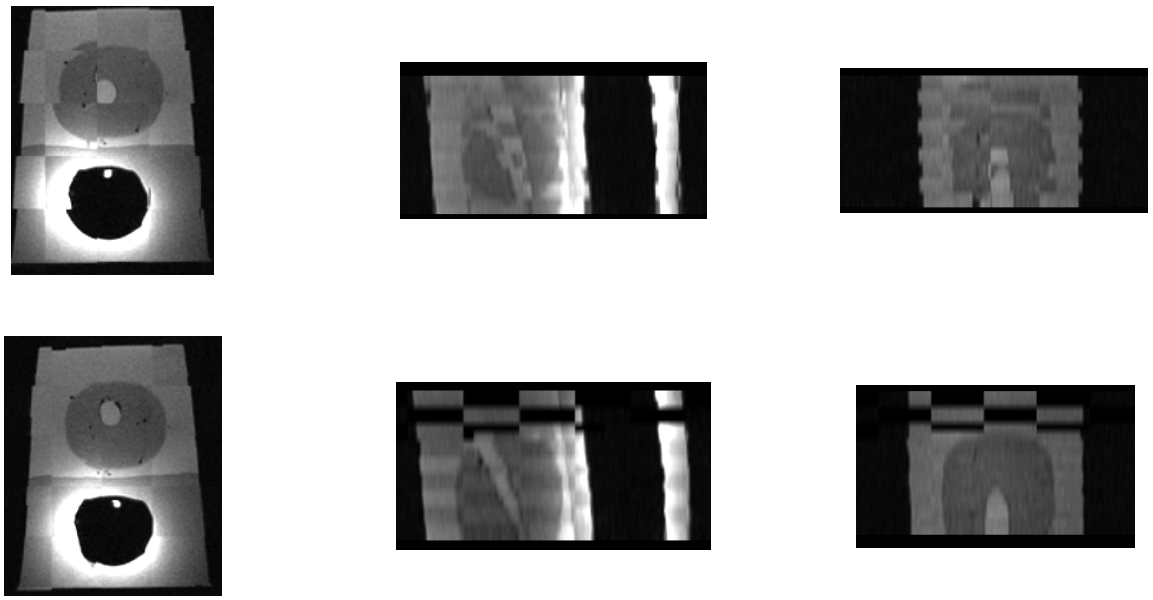

Figure 4: Checkerboard overlay of pre-op and intra-op phantom volumes. Views: Transverse(left), Sagittal(Middle), Coronal(Right). Top row: Before registration. Bottom Row: After Registration.

The registration took on average 39s for the patient simulations and 42s for the phantom experiments, depending on the number of restarts and the initial perturbation. For comparison purposes, we resampled the volumes to make the voxels isotropic (i.e. the spacing was changed from 0.625 x 0.625 x 3(or 4) to 0.625 x 0.625 x 0.625) but the registration time was doubled and the accuracy was worse. Thus, the results for isotropic volumes are not presented here, as this option was not investigated further. The mean registration error was 0.66mm ± 0.67 mm at a success rate of 95% out of the 100 patient simulation tests, where success was defined as a registration error less than 2mm. The overall registration error

for the phantom experiment was 1.64mm. Two of the six actual[3] registration tests were excluded from the results due to a high initial registration error (16mm and 22.4mm), which resulted in a high final registration error (4.7mm and 5.8mm). It was reasonable to dismiss these cases from the results since it is assumed that in the clinical situation, the prostate will not be displaced by more than roughly 10mm. The fourth phantom test case (fourth column of table 2) was included in the results since the initial displacement was close to 10mm and it allowed for testing the limits of the algorithm.

Table 1: Mean Registration Error ± Standard Deviation for Simulation Registrations					
Patient	**Patient 1**	**Patient 2**	**Patient 3**	**Patient 4**	**Overall**
RE ± Std Dev (mm)	0.87 ±0.80	0.29 ± 0.45	0.59 ±0.32	0.89 ±1.09	**0.66 ± 0.67**
Success Rate (%)	88	100	100	92	**95**

Table 2: Mean Registration Error for Phantom Registrations					
Initial RE (mm)	3.50	5.81	5.97	12.32	**Overall**
Final RE (mm)	0.75	0.86	1.38	3.58	**1.64**

5. DISCUSSION

The restart routine proved to be stable by demonstrating through the registration tests that all 100 patient simulation tests and the 75 phantom convergence tests converged to less than 2mm error within maximum of 5 restarts. The higher registration error for the phantom experiment was expected for two reasons: difference in intensity ranges of the fixed and moving images and the nature of the image. The difference in the intensity range of the intra-op and pre-op volumes may have been caused by the MRI operator using different imaging parameters of the MRI scanner for each volume acquisition. However, the effect of this difference on the registration was reduced by rescaling the volumes to the same range (8-bit grayscale) prior to registration. The second important factor that presented a difficulty for the phantom registration was the nature of the images themselves. The only features the registration can use to align the volumes are the ellipsoid (the prostate phantom) and a section of the black cylindrical whole (imitating a rectum). On the other hand, the prostate has visible blood vessels which allow the algorithm to clearly distinguish one slice from another, while the phantom has no interior features to help the registration. Figure 5 shows transverse samples of the images used in the simulation and phantom tests. It is clear that the simulated patient image contains more features, making registration a relatively easier task. Nevertheless, the mean registration error of the four phantom tests arrived at 1.64mm, which is below the 2mm tolerance.

Figure 5: Sample transverse slices of (left) patient intra-op volume and (right) phantom intra-op volume cropped to the prostate VOI.

[3] "Actual" refers to the use of real intra-op slices rather than simulated intra-op slices

6. CONCLUSION

Our results show that the high-resolution slice to volume approach to intra-op prostate tracking is feasible given that the algorithm can track the prostate to within an error of 2mm spherical radius around the target point. Our clinical objective of accuracy was met through demonstration of both simulation tests (0.66mm) and phantom tests (1.64mm). As for the speed objective, our simulation tests resulted in a registration time (39s) faster than previous groups'. Given the inevitable difficulties in registering phantom volumes as discussed previously, the registration time is reasonable (42s). The simulation and phantom results prove that MRI-guided prostate tracking has a promising future, with hopes of improving needle placement accuracy. With the high degree of accuracy obtained from this study, we anticipate that our rigid registration algorithm will be able to also register prostate images that feature edematic deformation. The next step in this project is to use actual pre needle insertion and post needle insertion MR images of the patient to test our tracking algorithm.

ACKNOWLEDGMENTS

This work has been supported by the National Institute of Health under grants 5R01CA111288-04 and 5R01EB002963-05. The patient image data were taken from an image database that was generously shared by our colleagues at U.S. National Institutes of Health. The phantom image data were taken from our colleague, Denis Suljendic, at Princess Margaret Hospital, Toronto, Canada.

REFERENCES

[1] Ladd, M. E., Quick, H. H. & Debatin, J. F. "Interventional MRA and intravascular imaging", *J Magn Reson Imaging* 12, 534-46. (2000).

[2] Quesson, B., de Zwart, J. A. & Moonen, C. T. "Magnetic resonance temperature imaging for guidance of thermotherapy", *J Magn Reson Imaging* 12, 525-33. (2000).

[3] Lewin, J. S., Metzger, A. & Selman, W. R. "Intraoperative magnetic resonance image guidance in neurosurgery", *J Magn Reson Imaging* 12, 512-24. (2000).

[4] Hata, N., Tokuda, J., Morikawa, S. and Dohi, T. "Projection Profile Matching for Intraoperative MRI Registration Embedded in MR Imaging Sequence" MICCAI 2002, pp. 164–169, (2002)

[5] Fei, B., Duerk, J. L, Boll, D. T., Lewin, J. S. and Wilson, D. L., "Slice-to-Volume Registration and its Potential Application to Interventional MRI-Guided Radio-Frequency Thermal Ablation of Prostate Cancer", IEEE TRANSACTIONS ON MEDICAL IMAGING, VOL. 22, NO. 4, APRIL (2003)

[6] Chandler, A.G., Pinder, R.J., Netsch, T., Schnabel, J.A., Hawkes, D.J., Hill, D.L.G. and Razavi, R., "Correction of Misaligned Slices in Multi-Slice MR Cardiac Examinations by Using Slice-to-Volume Registration", 3rd International Symposium on Biomedical Imaging: Nano to Macro, pp. 474-477. (2006).

[7] Gill, S., Abolmaesumi, P., Vikal, S., Mousavi, P. and Fichtinger, G., "Intraoperative Prostate Tracking with Slice-to-Volume Registration in MR", 20th International Conference of the Society for Medical Innovation and Technology, Vienna, Austria 2008, Electronic Proceedings, ISBN 3-902087-25-0, pp. 154-158, (2008)

[8] http://www.upmccancercenters.com/cancer/prostate/biopsyneedle.html

[9] Edurado, I. C., Singh, H., Shariat, S.F., Kadmon, D., Miles, B.J., Wheeler, T.M., and Slawin, K.M., "EFFECTS OF SYSTEMATIC 12-CORE BIOPSY ON THE PERFORMANCE OF PERCENT FREE PROSTATE SPECIFIC ANTIGEN FOR PROSTATE CANCER DETECTION", The Journal of Urology, Vol. 172, 900–904, (2004)